Dissertation

Role of the scaffolding protein JLP in UVB-induced apoptosis

Graduate School of
Natural Science &Technology
Kanazawa University

Division of Life Sciences
D-3 Course: Genetic Information

1023032526
Enkhtuya Radnaa

Chief Advisor
Prof. Dr. Katsuji Yoshioka
Division of Life Sciences, Kanazawa University, Japan

CONTENTS

ACKNOWLEDGEMENTS

My sincere gratitude goes to my supervisor Prof. Dr. Katsuji Yoshioka, Division of Molecular Cell Signaling, Cancer Research Institute, Kanazawa University, for his special guidance and encouragement in the successful completion of this research. I am deeply grateful for his good supervision and constructive comments.

I would like to express heartfelt thanks to Dr. Tokiharu Sato, Division of Molecular Cell Signaling, Cancer Research Institute, Kanazawa University, for his contribution to this research, valuable suggestions and critical comments.

I am very thankful to Drs. Mitsuo Wakasugi and Tsukasa Matsunaga, Graduate School of Natural Science and Technology, Kanazawa University, for their collaboration in DNA repair assay of this work.

To all lab members, it has been a pleasure and good experience studying in a supportive, friendly environment.

Finally, my special gratitude goes to my husband who gave me all the strengths and encouragements during this whole time. It would not be possible to complete this work without his help and support.

ABSTRACT

Ultraviolet B (UVB) component of sunlight causes many adverse biological effects, including apoptosis, and eventually can lead to skin cancer. Growing evidence indicates that the UVB-induced signaling network is complex and involves diverse cellular processes. In this study the role of c-Jun NH_2-terminal kinase-associated leucine zipper protein (JLP), a scaffold protein for mitogen-activated protein kinase (MAPK) signaling cascades, was investigated in UVB-induced apoptosis. I found that UVB-induced skin epidermal apoptosis was reduced in *Jlp* knockout (KO) as well as in keratinocyte-specific *Jlp* KO mice compared to those of the controls. While exploring molecular mechanisms of the diminished apoptosis in *Jlp*-deficient mice, it was revealed that UVB-induced DNA repair system shows no evidence for the involvement of JLP in this process; however, UVB-stimulated p38 MAPK activation was impaired in both *Jlp* KO and keratinocyte-specific *Jlp* KO mice. Moreover, topical treatment of UVB-irradiated mouse skin with a p38 inhibitor significantly suppressed the epidermal apoptosis in wild-type mice, but not in *Jlp* KO mice. These findings suggest that JLP in skin basal keratinocytes plays an important role in UVB-induced apoptosis by modulating p38 MAPK signaling pathways. This is the first study to demonstrate a critical role for JLP in an *in vivo* response to environmental stimulation.

ABBREVIATIONS

6-4PP	(6-4) photoproducts
BCA	bicinchoninic acid
BPE	bovine pituitary extract
BSA	bovine serum albumin
cKO	conditional KO
CPD	cyclobutane pyrimidine dimers
CPDs	cyclobutane pyrimidine dimers
DAPI	4', 6-diamidino-2-phenylindole
dNTPs	deoxyribonucleotides
EDTA	ethylenediaminetetraacetic acid
ERK	extracellular signal-regulated kinase
EtOH	ethanol
HRP	horseradish peroxidase
JIP	JNK-interacting protein
JLP	c-Jun NH_2-terminal kinase-associated leucine zipper protein
JNK	c-Jun NH_2-terminal kinase
JSAP1	JNK/stress-activated protein kinase-associated protein 1
K5-Cre	Keratin5-Cre
KO	knockout
MAPK	mitogen-activated protein kinase
MeOH	methanol
NP-40	nonidet p-40
OTC	optimal cutting temperature

PAGE	polyacrylamide gel electrophoresis
PB	phosphate buffer
PCR	polymerase chain reaction
PFA	paraformaldehyde
PVDF	polyvinylidene fluoride
R26R	rosa26-lacz reporter
RIPA	radioimmunoprecipitation assay
ROS	reactive oxygen species
rpm	rotations per minute
SDS	sodium dodecyl sulfate
SEM	standard error of the mean
SPAG9	sperm associated antigen 9
SPF	specific pathogen free
TBS	tris-buffered saline
TBST	tris-buffered saline tween
TEMED	tetramethylethylenediamine
UVB	ultraviolet B
UVR	ultraviolet radiation
X-gal	5-Bromo-4-Chloro-3-Indolyl-β-D-Galactoside

INTRODUCTION

We are constantly exposed to environmental hazards, and our first protective barrier is the skin. It protects us against water loss and external physical, chemical, and biological insults, such as wounds, ultraviolet radiation (UVR), and microorganisms (Lippens *et al*., 2009). Among them UVR elicits many adverse effects in the skin including erythema, aging, cell death (apoptosis), and skin cancer (Tobin *et al*., 1998). UVB (280-320 nm) of UVR is mostly absorbed in the epidermis of the skin, and induces DNA photolesions, such as cyclobutane pyrimidine dimers (CPD) and (6-4) photoproducts (6-4PP), which, if inefficiently repaired result in deleterious mutations. When DNA damage is too extensive to be repaired, apoptosis is induced. This is a protective mechanism that eliminates any altered cells from the skin. UVB irradiation also induces alterations in gene expression that are mediated by signaling molecules, including mitogen-activated protein kinases (MAPKs) (Bode & Dong, 2003; Bowden, 2004). Growing evidence indicates that the UVB-induced signaling network is complex and involves diverse cellular processes, such as apoptosis and survival. To date, the mechanisms involved in regulating UVB-induced apoptosis pathways remain unclear. Mammalian MAPK signaling cascades, consisting of MAPK kinase kinase, MAPK kinase, and MAPK, play crucial roles in multiple cellular processes, including cell proliferation, differentiation, and apoptosis. Three MAPK subfamilies have been extensively studied: extracellular signal-regulated kinase (ERK), c-Jun NH_2-terminal kinase (JNK), and p38 MAPKs. ERK MAPKs primarily respond to mitogenic and differentiation stimuli, while JNK and p38 MAPKs are strongly activated by inflammatory signals and stress, including UVR. The mammalian MAPK signaling system employs scaffold proteins, in part, to organize the MAPK signaling components into functional modules, thereby enabling the efficient activation of specific MAPK cascades. To date, nearly 20 proteins have been identified as scaffold factors for mammalian MAPK signaling pathways. (Enkhtuya *et al*., in press). JLP was originally identified as a binding protein for the transcription factor Max, and further biochemical study indicated that JLP functions as a scaffold protein for the JNK and p38 MAPK signalling modules (Lee *et al*., 2002).

JLP, one of the three known splice variants of *Jip4* gene (other 2 splice variants are JIP4 and SPAG9) (Kelkar *et al*., 2005), is expressed in most tissues from murine, with highest expression level in the testis, moderate or low expression level in the brain, lung, spleen, and ovary, and very low expression level in the heart, liver, kidney epididymis, and uterus according to Iwanaga *et al*. by western blot analysis (Iwanaga *et al*., 2008). Studies of JLP have mainly focused on identifying its interacting proteins, which include kinesin light chain 1 and Ga13, the α-subunit of the heteromeric G13 protein (Nguyen *et al*., 2005; Kashef *et al*., 2005). JLP has also been reported to play an important role in myogenesis by interacting with the cell-surface protein Cdo (Takaesu *et al*., 2006). In 2008, Iwanaga *et al.* reported that JLP-null mice are viable and grow normally, but exhibit reduced male fertility (Iwanaga *et al*., 2008). However, the *in vivo* functions of scaffolding protein JLP remain largely unknown.

To better understand the complex UVB response, in this study I investigated the function of JLP in UVB-induced apoptosis in the skin by analyzing *Jlp*-deficient mice. The results suggest that JLP plays an important role in this apoptosis by modulating p38 MAPK signaling cascades.

MATERIALS AND METHODS

Mice

All the experiments involving animals were conducted according to Institutional Animal Care and Use Committee of Kanazawa University. Mice used in this study were housed under SPF (Specific Pathogen Free) conditions at the Institute for Experimental Animals, Advanced Science Research Center, Cancer Research Institute, Kanazawa University. Light regime was 12 hours of light per day. 4 weeks old offspring were ear-marked and tail tips were cut for genotype analysis. In this study, previously generated *Jlp*$^{-/-}$ mice, by Iwanaga *et al,* were used (Iwanaga *et al*., 2008). For generation of keratinocyte specific conditional *Jlp* knockout mice, two loxP sites were inserted to flank exon 5 of the *Jlp* gene. These mutant mice were backcrossed to C57BL/6 for more than ten generations, and the resulting mice were crossed with *Keratin5-Cre* (*K5-Cre*) transgenic mice. C57BL/6 mice were obtained from Japan SLC (Hamamatsu, Japan), *K5-Cre* transgenic mice (Tarutani *et al*., 1997) from the Center for Animal Resources and Development of Kumamoto University, and *R26R* mice from the Jackson Laboratory (Bar Harbor, ME, USA).

Isolation of genomic DNA & Mice genotyping

Genomic DNA for mice genotyping was extracted from clipped tails. Tissue fragments were placed in 1.5 ml tubes and incubated in 100 µl lysis solution for 30 minutes at 95°C. Lysates were placed on ice for 3 minutes and centrifuged for 1 minute at 13'000 rpm. Upon centrifuge, 100 µl neutralization solution was added to the lysates and mixed well. The lysates were centrifuged for 5 minutes at 13'000 rpm and the supernatant was transferred to a new 1.5 ml tube with equal volume of chloroform and mixed vigorously. After centrifuging for 15 minutes at 13'000 rpm, upper phase containing genomic DNA transferred to a new 1.5 ml tube. Lysates were stored at – 20°C or directly processed.

Lysis solution (pH 12.0)
25 mM NaOH

Neutralization solution (pH 5.0)
40 mM Tris-HCI

0.2 mM EDTA

Genotyping of mice was routinely performed by PCR analysis. Genomic DNA was amplified in following PCR conditions with following specific primers.

PCR program for *jlp* gene:

Denature DNA	94˚C for 20 seconds
Primer annealing	58.5˚C for 30 seconds
Extension	72˚C for 60 seconds

These steps are repeated 30 times.

PCR program for *Cre* recombinase gene:

Denature DNA	94˚C for 20 seconds
Primer annealing	62˚C for 30 seconds
Extension	72˚C for 30 seconds

These steps are repeated 30 times.

Primers for disruption of *jlp* gene:

Primer 1 (*Jlp*-G53): 5'-TGTCAGTTCCGCTGGCTTCGGTA-3' (for wild-type allele)
Primer 2 (neoH): 5'-CTCAGCCTGCAGGCTAAAATCCTG-3' (for knockout allele)
Primer 3 (*Jlp*-G52): 5'-TAAAGCGCATGCTCCAGACTGCCTT-3' (for wild-type and knockout allele)

Primers for conditionally disrupted *jlp* gene:

Primer 1 (GCK36): 5'-GTTTCCGTGTTCATTAGGGTGTGTTCAC-3'
Primer 2 (GCK37): 5'-CCCATGTAAGAGCAACACAGTTCTTACC-3'

Primers for *Cre* recombinase gene:

Primer 1 (*Cre*-s-F): 5'-ACCTGATGGACATGTTCAGGGATCG-3'
Primer 2 (*Cre*-s-R): 5'-TCCGGTTATTCAACTTGCACCATGC-3'

After the reaction was finished, the samples were analyzed by 1.5% agarose gel electrophoresis for 30 minutes or 60 minutes at 100 Voltages.

Genotyping PCR-reaction mix:

DNA template	*2.0 µl*
Primer F (10 µmol)	*1.0 µl*
Primer R (10 µmol)	*1.0 µl*
PCR buffer (10 x)	*4.0 µl*
2 mM dNTP	*2.0 µl*
Go Taq DNA Poly (5 U/µl)	*0.1 µl*
ddH_2O	*10.0 µl*
Total	***20 µl***

UVB Irradiation and Treatment with a Pharmacological p38 Inhibitor

The hair of back skin was shaved by a hair clipper (Panasonic ER 503 PP) and remaining hair was removed by a shaver (Panasonic ES 3832 P) 24 hours before the experiments. On the next day, the deeply anesthetized mice (intraperitoneal injection of pentobarbital sodium, 60 mg/kg) were irradiated by 2.8 kJ/m^2 dose of UVB with the use of CL-1000 ultraviolet crosslinker (UVP, Inc. Upland, CA, USA). For the topical inhibition of p38 MAPK, SB203580 (#13067; Cayman Chemical, Ann Arbor, MI, USA) was dissolved in acetone and used at a dose of 0.5 µmol. The inhibitor was reconstituted immediately before use and applied in a volume of 40 µL to the dorsal skin for 1 hour before irradiation and immediately following irradiation.

Histological Analysis, Immunofluorescence, and β-Galactosidase Staining

Sample preparation

Adult mice were anesthetized and fixed by transcardial perfusion with 4% paraformaldehyde (PFA)/ 0.1 M PB. Back skin was taken and placed in a fresh 4% PFA/ 0.1M PB for post fixation at 4°C, overnight. Fixed skin sections were treated

with 10% sucrose/ 0.1M PB for 2 hours, 20% sucrose/0.1 M PB for 6 hours and 30% sucrose/ 0.1M PB at 4˚C for overnight for cryoprotection. Following day, skin samples were embedded in OTC compound (Sakura Finetek, Tokyo, Japan). Frozen blocks were stored at – 80˚C for further usage.

Hematoxylin and Eosin staining

Frozen blocks were warmed up at – 20˚C before the experiments. 7-µm sections were cut with a cryotome (Sakura Tissue Tek Cryo 3, cryostat), collected on micro slide glasses (Matsunami, S 9441), air-dried for 40 minutes at room temperature. Sections were washed by 1 x TBST 2 times for 5 minutes, rinsed in tap water for 1 minute. After staining in hematoxylin for 5 minutes, sections were rinsed in tap water for 5 minutes. Then sections were stained in eosin for 5 minutes, rinsed in tap water 5 minutes and dehydrated in 50% EtOH, 70% EtOH, 90% EtOH and 95% EtOH serially for 1 minute for each. After clearing in xylen for 1 minute, sections were mounted by mount-quick (Daido Sangyo, Tokyo, Japan).

Immunohistochemical staining

20-µm frozen sections were air-dried as described above and washed by 1 x TBST 2 times for 5 minutes. Sections were surrounded by pap pen (liquid blocker, Daido Sangyo, Tokyo, Japan), incubated at first with blocking buffer for 1 hour at room temperature and next with the primary anti-active caspase-3 antibody for overnight at 4˚C. Following day, sections were washed by 1 x TBST 3 times for 5 minutes and incubated with Alexa-labeled secondary antibodies for 3 hours at room temperature, followed by nuclear staining with 4,6-diamidino-2-phenylindole (DAPI; Sigma, St Louis, MO, USA) for 10 minutes. Sections were washed by 1 x TBST 3 times for 5 minutes and mounted with 80 % glycerol.

For phosphorylated and activated p38 (p-p38) immunostaining, back skin was removed from deeply anesthetized mice, embedded in OCT compound, and frozen in liquid nitrogen. 20-µm frozen sections were fixed in 4% PFA/ 0.1M PB for 10 minutes and subjected to immunohistochemical analysis as described above.

0.2 M phosphate buffer (PB) (pH 7.4)

*NaH_2PO_4 * 2 H_2O*	*2.96 g*
*Na_2HPO_4 * 12 H_2O*	*29 g*
dH_2O	*up to 500 ml*

TBS (10 x) (pH 7.4)

Tris base	*30.0 g*
NaCl	*80.0 g*
KCl	*2.0 g*
dH_2O	*up to 1000 ml*

TBST (1 x)

10 x TBS	*100 ml*
Tween 20	*1 ml*
dH_2O	*up to 1000 ml*

Blocking buffer

2 % BSA (bovine serum albumin)
2 % goat serum
0.4 % triton – x 100 in 1 x TBST

β-galactosidase staining

R26R mice were mated with K5-Cre mice and offspring at postnatal day (P) 5 were deeply anesthetized, and the back skin was removed, fixed in 4% PFA/ 0.1M PB, cryoprotected as described above, and embedded in OCT compound. 20-μm frozen sections were stained in PBS containing 1 mg/mL X-gal (5-Bromo-4-Chloro-3-Indolyl-β-D-Galactoside; Takara Bio, Otsu, Japan), 2 mM $MgCl_2$, 5 mM potassium ferrocyanide and 5 mM potassium ferricyanide for 24 hours at 37˚C. Samples were dehydrated in 50% EtOH, 70% EtOH, 90% EtOH and 95% EtOH serially for 1 minute for each. After clearing in xylen for 1 minute, sections were mounted by mount-quick.

The following primary antibodies were used: anti-active caspase-3 antibody (1:600; #9661; Cell Signaling, Boston, MA, USA) and anti-p-p38 antibody (1:1600; #4511; Cell Signaling). Secondary antibodies were Alexa fluor 488- (#A11008) and 568-conjugated (#A11011) antibodies (both diluted at 1:1000; Invitrogen, Rockville, MD, USA). Fluorescence images were captured with a confocal laser-scanning microscope (LSM510 META, Carl Zeiss, Oberkochen,

Germany). Other images were captured with a fluorescence microscope (BX50, Olympus, Tokyo, Japan).

Western Blotting

Sample preparation

Back skin was removed from deeply anesthetized mice, snap frozen in liquid nitrogen. Frozen skin was pulverized with a mortar and pestle. The pulverized skin was collected into 1.5 ml tube and added lysis buffer. After sonification, lysates were centrifuged at 13,000 rpm for 20 minutes. Supernatants were collected into new 1.5ml tube and protein concentration was determined using the BCA protein assay kit (#23225, Thermo Scientific, MA, USA). SDS-sample buffer was added into cell lysates and stored at – 20˚C for further usage. Primary keratinocytes were also lysed by same procedure.

RIPA buffer
50mM Tris-HCl (pH 8.0)
150mM NaCl
1% NP-40
0.5% Sodium deoxycholate
0.1% SDS

Lysis buffer was prepared by adding protease and phosphatase inhibitors into RIPA buffer just before use.

SDS-Sample buffer
250 mM Tris-HCl (pH 6.8)
10 % SDS
30 % Glycerol
5 % β – mercaptoethanol
0.02 % Bromophenol blue

SDS-PAGE running

Proteins were separated elecrophoretically according to their molecular weight in SDS-polyacrylamide gels. Gels consisted of stacking (5% acrylamide) and

separating parts (8 % or 12 % acrylamide). 20 µg or 50 µg protein lysates, incubated at 95°C for 5 minutes, were loaded into the wells. Electrophoresis was carried out until bromophenol blue reached the bottom of the separating gel, which was about 65 minutes (300 V, 30 mA).

Separating gel (8 % / 12 %)	
Solution components	*10.0 ml*
H_2O	*4.6 ml / 3.3 ml*
30 % acrylamide mix	*2.7 ml / 4.0 ml*
1.5 M Tris (pH 8.8)	*2.5 ml*
10 % SDS	*0.1 ml*
10 % ammonium persulfate	*0.1 ml*
TEMED	*0.006 ml/0.004 ml*

for 1 gel 5.2 ml of mixture was used.

Stacking gel (5 %)	
Solution components	*3.0 ml*
H_2O	*2.1 ml*
30 % acrylamide mix	*0.5 ml*
1.0 M Tris (pH 6.8)	*0.38 ml*
10 % SDS	*0.03 ml*
10 % ammonium persulfate	*0.03 ml*
TEMED	*0.003 ml*

for 1 gel 1.2 ml of mixture was used.

Running buffer (1 x)

Tris base	*30.2 g*
Glycine	*144.0 g*
SDS	*10.0 g*
dH_2O	*up to 10 l*

Transfer of proteins to the membrane

Separated proteins were transferred to a PVDF membrane (# IPVH00010, Merck Milipore, MA, USA) using Trans-Blot electrophoretic transfer cell (BE – 351, Bio Craft, Michigan, USA). The membrane was activated with MeOH (20 seconds), rinsed with water for 2 minutes. Transfer sandwich was assembled and the cassette was placed in an electrode module. The blotting was conducted for 95 minutes (300 V, 100 mA). After finishing, the sandwich was disassembled and the membrane was washed by 1 x TBST for 10 minutes.

Transfer buffer (1 x)

Tris base	*30.29 g*
Glycine	*144.13 g*
Methanol	*2.0 l*

Protein detection on the membrane

The membrane was blocked with 5 % non-fat milk (Skim Milk Powder) (#190-12865, Wako Pure Chemical Industries, VA, USA) for 60 minutes at room temperature. Primary antibodies were generally diluted in a respective blocking buffer (only for phosphorylated protein detection, 5% BSA was used) and incubated at 4˚C for overnight. The following day, the membrane was washed 2 times for 10 minutes and incubated for 2 hours at room temperature with the appropriate HRP-conjugated secondary antibody diluted in 5 % non-fat milk. The membrane washed 3 times for 10 minutes and proteins were visualized with the Immobilon Western Chemiluminescence HRP Substrate (Millipore, Billerica, MA, USA). The signal was captured by Image Quant^{TM} Las 4000 (GE Healthcare, Life Sciences, Buckinghamshire, UK).

Following antibodies were used: anti-JLP (Iwanaga *et al*., 2008; Gantulga *et al*., 2008) (2 µg ml-1), anti-p-JNK (#9251), anti-pan-JNK (#9258), anti-p-p38 (#4631), anti-pan-p38 (#9212), anti-p-ERK (#4377), anti-pan-ERK (#9102) (all diluted at 1:1000; Cell Signaling), and anti-α-tubulin (1:5000; #T5168; Sigma) antibodies.

Primary keratinocytes

P0 or P1 newborn pups were killed by decapitation, and the back skin was removed and incubated with CnT-57 medium (CELLnTEC, Berne, Switzerland) containing 5 mg/ml dispase (Invitrogen, Rockville, MD, USA) and 2 x antibiotics/ antimycotics (CnT-ABM) (CELLnTEC) at 4˚C for overnight. The epidermis was separated from the dermis and incubated with TrypLE Select (Invitrogen) for 30 minutes at room temperature. Separated keratinocytes were then collected by centrifugation and seeded at a density of 3 x 10^4 cells/ cm^2 in CnT-57 medium containing supplements (CnT-57.A, CnT-57.B, CnT-57.C and Bovine Pituitary Extract (BPE)) in 35 mm culture dishes. Cells were cultivated at the condition of 37˚C, 5% CO_2 and fresh medium were replaced every other day. Subconfluent passage 1 cells were used for experiments.

Measurement of 6-4PP repair

In collaboration with Drs. Wakasugi and Matsunaga, an assay for DNA repair system was performed. Appropriate numbers of keratinocytes from *Jlp*$^{+/-}$ or *Jlp*$^{-/-}$ mice were plated in 35-mm glass-bottom dishes, and then UVB-induced 6-4PP lesions were measured as previously described (Wakasugi *et al*., 2009), using the 6-4PP-specific antibody, 64M-5 (Mori *et al*., 1991). Immunofluorescence images of labeled 6-4PP lesions were obtained using the All-in-One fluorescence microscope BZ-9000 (Keyence, Osaka, Japan), and 6-4PP levels were calculated from the fluorescence intensities measured using ImageJ software (National Institutes of Health, Bethesda, MD, USA).

Statistical analysis

Significance was determined using the two-tailed unpaired Student's *t*-test. Values of $P < 0.05$ were considered to be statistically significant.

RESULTS

Phenotypic and histological analysis of *Jlp*$^{-/-}$ mice

Jlp$^{-/-}$ mice were previously generated by targeted gene disruption using 129-derived ES cell lines (Iwanaga *et al*., 2008). Even after extensive backcrossing (more than 10 times) onto the C57BL/6 background, *Jlp*$^{-/-}$ mice exhibited a lightened coat color and pale skin (Fig. 1A), as reported for homozygous dazzle mice (Krebs and Beutler, 2010). The dazzle mouse was generated by N-ethyl-N-nitrosourea mutagenesis on the C57BL/6 background and contains a missense mutation in the *Jlp* gene (Krebs and Beutler, 2010). Taken together, these results indicate that the pigmentation defects can be attributed to the loss of normal JLP function. However, there were no obvious histological differences observed in the skin between control (*Jlp*$^{+/-}$), and *Jlp*$^{-/-}$ mice (Fig. 1B).

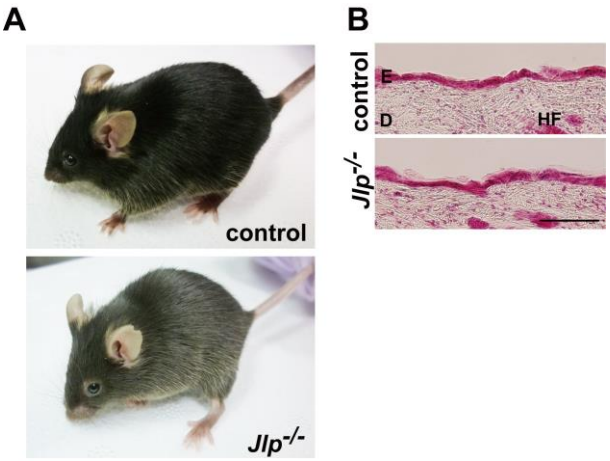

Figure 1. Phenotypic and histological analysis of *Jlp*$^{-/-}$ mice. **(A)** Macroscopic appearance of control (*Jlp*$^{+/-}$) and *Jlp*$^{-/-}$ adult mice. **(B)** Hematoxylin and eosin staining of 7-µm-thick frozen sections from the shaved back skin of control and *Jlp*$^{-/-}$ adult mice. The images were captured by an Olympus BX50 microscope with a 20x objective. E, epidermis; D, dermis; HF, hair follicle. Scale bar, 100 µm.

Jlp-deficient mice exhibit decreased apoptosis in response to UVB irradiation

Next the effect of *Jlp* deficiency on UVB-induced apoptosis in mouse skin was examined. To this end, immunohistochemical analysis using an antibody against active caspase-3, a well-known apoptotic marker, was performed. Upon UVB exposure, the number of active caspase-3-positive cells, which were detected mostly in the epidermis (Fig. 2A) was significantly decreased in *Jlp*$^{-/-}$ compared with control

mice (Fig. 2B). These results suggested that JLP is a positive regulator of UVB-induced apoptotic pathways.

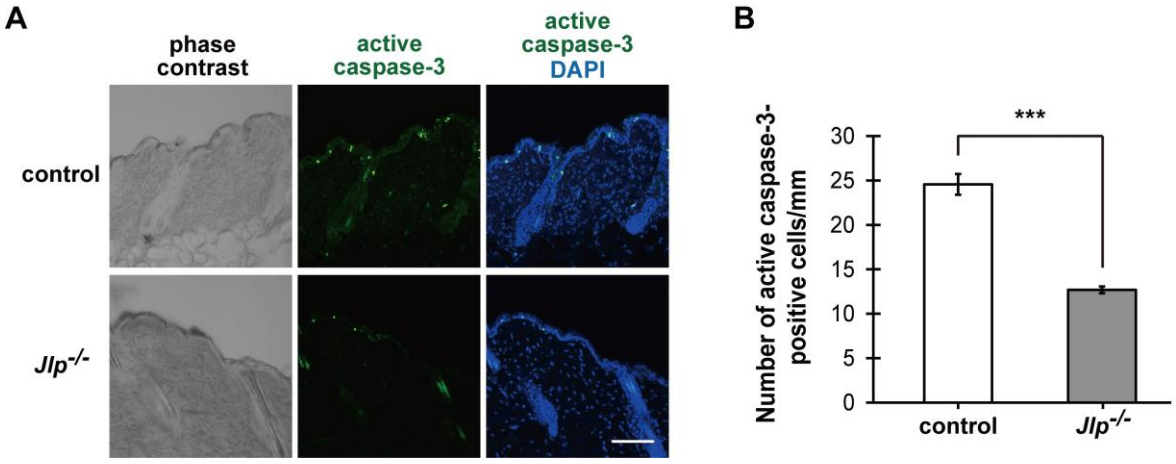

Figure 2. JLP ablation reduces UVB-induced apoptosis in mice. **(A)** Immunohistochemical staining for active caspase-3 in control (*Jlp*$^{+/-}$) and *Jlp*$^{-/-}$ mice. The backs of control and *Jlp*$^{-/-}$ adult mice were shaved and irradiated with 2.8 kJ/m^2 of UVB. After 24 hours, skin samples were obtained and fixed, and 20-µm-thick frozen sections were stained with an anti-active caspase-3 antibody and DAPI. The images were captured by a Zeiss LSM510 META confocal microscope with a 20x objective. Scale bar, 100 µm. **(B)** Quantification of the results in A. The number of active caspase-3-positive cells in the epidermis was counted over a linear distance of 20-30 mm, and averaged for each 1-mm interval. Values are the mean + SEM from three independent experiments. ***P < 0.001.

Effect of *Jlp* deficiency on the repair of UVB-induced DNA damage

To gain insight into the mechanisms underlying the attenuated UVB-induced apoptosis in *Jlp*-deficient mice, the DNA repair capability of keratinocytes lacking JLP was investigated. The repair of 6-4PPs, which a useful indicator for evaluating DNA repair compared to CPDs because of their quicker and effective excisions from UV-irradiated cellular DNA, was investigated (Mitchell *et al*., 1985; Mizuno *et al*., 1991). The 6-4PP repair in epidermal keratinocytes prepared from the control and *Jlp*$^{-/-}$ mice was examined over time. After UVB exposure, the 6-4PP lesions were removed with similar kinetics in the control and *Jlp*$^{-/-}$ keratinocytes (Fig. 3), suggesting that JLP is not involved in the DNA excision repair of UVB-induced

damage, and furthermore that the inhibition of apoptosis observed in *Jlp*$^{-/-}$ mice is not due to a decreased accumulation of DNA damage.

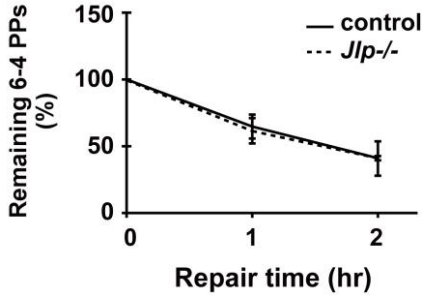

Figure 3. Kinetics of 6-4PP repair in *Jlp-/-* keratinocytes. Primary keratinocytes derived from control (*Jlp*$^{+/-}$) and *Jlp*$^{-/-}$ P0 mice were irradiated with 160 J/m^2 of UVB. The cells were incubated for the indicated periods and processed for the detection of 6-4PP. Each point represents the mean + SEM from three independent experiments.

Impaired UVB irradiation-induced MAPK activation in *Jlp*$^{-/-}$ mice

Next question was whether JLP ablation perturbs the normal MAPK activation response to UVB irradiation. The UVB-induced levels of phosphorylated and activated JNK (p-JNK), p38 (p-p38), and ERK (p-ERK) in the skin of control and *Jlp*$^{-/-}$ mice was analyzed by Western blotting (Fig. 4A). While the p-ERK levels were similar between the control and *Jlp*$^{-/-}$ mice, modest and substantial decreases in the levels of p-JNK and p-p38, respectively, were observed in the skin samples of *Jlp*$^{-/-}$ mice (Fig. 4A, compare lanes 3 and 4). The UVB-induced p38 activation was further analyzed by immunohistochemistry. As shown in Figure 4B and C, the p-p38 immunopositive signals in the epidermis were significantly lower in *Jlp*$^{-/-}$ mice compared to control mice.

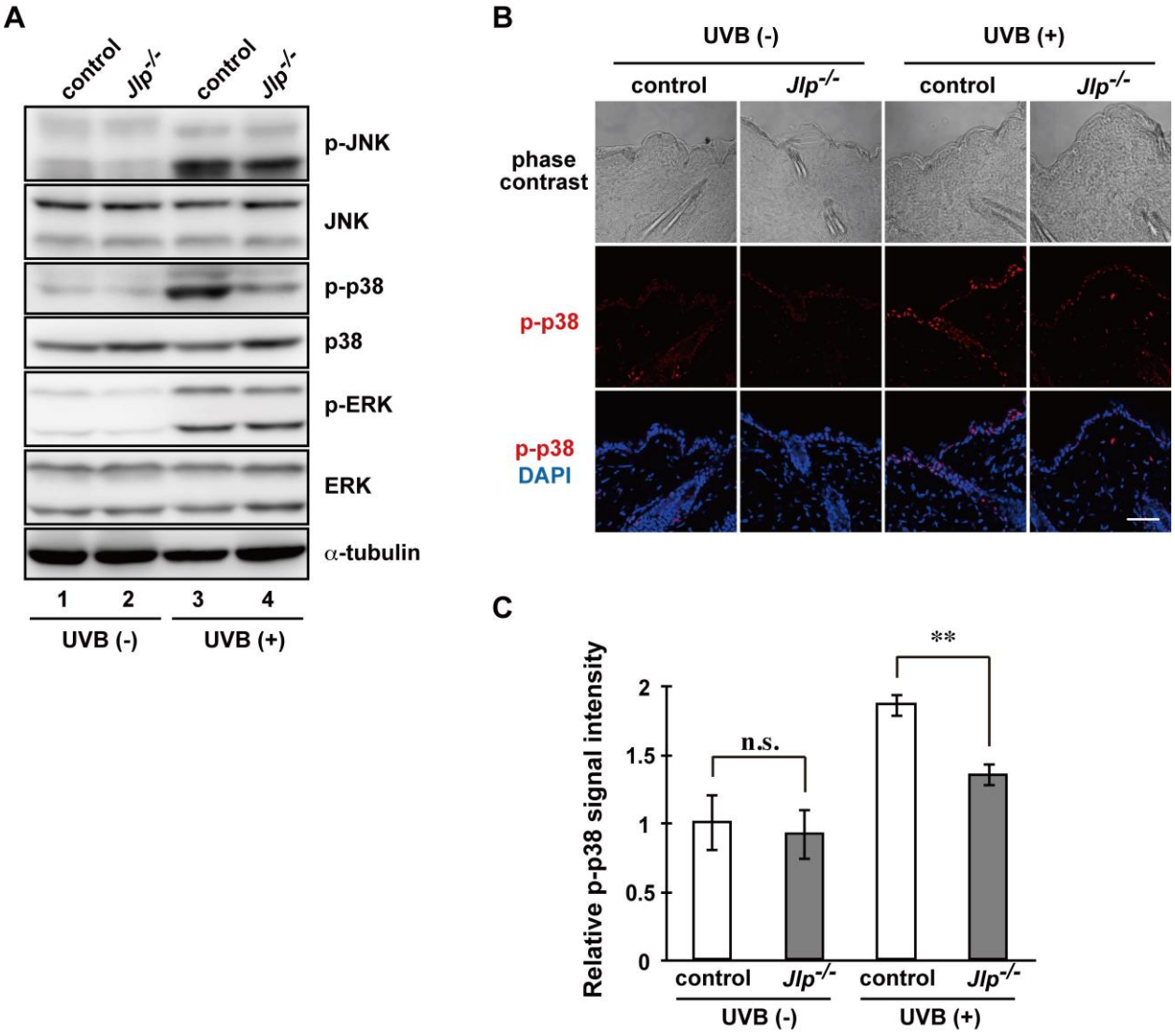

Figure 4. Impaired MAPK activation in the skin of *Jlp*$^{-/-}$ mice following UVB irradiation. **(A)** Western blotting analysis of MAPK activation in the skin of control (*Jlp*$^{+/-}$) and *Jlp*$^{-/-}$mice following UVB exposure. The backs of control and *Jlp*$^{-/-}$ adult mice were shaved and treated with (UVB (+)) or without (UVB (-)) 2.8 kJ/m^2 of UVB, as indicated. Thirty minutes after irradiation, cell lysates were prepared from the skin samples, and analyzed by Western blotting (50 µg lysate/lane) with the indicated antibodies. α-tubulin was used as a loading control. **(B)** Immunohistochemical staining for p-p38 in control (*Jlp*$^{+/-}$) and *Jlp*$^{-/-}$ mice. Control and *Jlp*$^{-/-}$ adult mice were shaved and treated with or without UVB as in A. Thirty minutes after irradiation, skin samples were obtained and fixed, and 20-µm-thick frozen sections were stained with anti-p-p38 antibody and DAPI. The images were captured by a Zeiss LSM510 META confocal microscope with a 40x objective. Scale bar, 50 µm. **(C)** Quantification of the results in B. The immunofluorescence signal intensity of p-p38 in the epidermal compartment approximately 0.2 mm^2) was quantified using ImageJ. The mean intensity per area of the untreated

Jlp$^{-/-}$, the irradiated control (*Jlp*$^{+/-}$), and the irradiated *Jlp*$^{-/-}$ mice was normalized to the mean intensity per area of the untreated control (*Jlp*$^{+/-}$) mice, respectively. Values are the mean + SEM from three independent experiments. n.s., not significant; **P < 0.01.

Generation and analysis of mice with a keratinocyte-specific deletion of JLP

To examine whether JLP expressed in skin basal keratinocytes is responsible for UVB-induced apoptosis, keratinocyte-specific *Jlp* conditional KO (cKO) mice were generated by crossing mice carrying *Jlp* loxP-flanked (floxed) alleles with Keratin5-Cre (K5-Cre) transgenic mice. The region-specific expression of Cre recombinase in the K5-Cre mice was confirmed using the *Rosa26-lacZ* reporter (*R26R*) (Fig. 5 B). The loss of JLP expression in keratinocytes was assessed by Western blotting of cell lysates prepared from primary keratinocytes isolated from control (*Jlp*$^{flox/+}$*;K5-Cre*) and *Jlp* cKO (*Jlp*$^{flox/flox}$*;K5-Cre*) mice (Fig. 5A). Results indicated that the *Jlp* gene was successfully disrupted in keratinocytes by K5-Cre-mediated recombination. The UVB-induced apoptosis and p38 MAPK activation in the control and *Jlp* cKO mice were then analyzed. Consistent with the findings in *Jlp*$^{-/-}$ mice (Fig. 2A, B), the *Jlp* cKO mice exhibited significantly decreased apoptosis in the epidermis in response to UVB irradiation, compared with control mice (Fig. 5C, D). Moreover, reduced levels of p-p38 were observed in the skin samples of *Jlp* cKO mice by Western blotting (Fig. 5E). The UVB-induced p38 activation was also analyzed by immunohistochemistry, and as a result the p38 immunosignals in the epidermis were found significantly lower in the *Jlp* cKO mice compared with control mice (Fig. 5F, G).

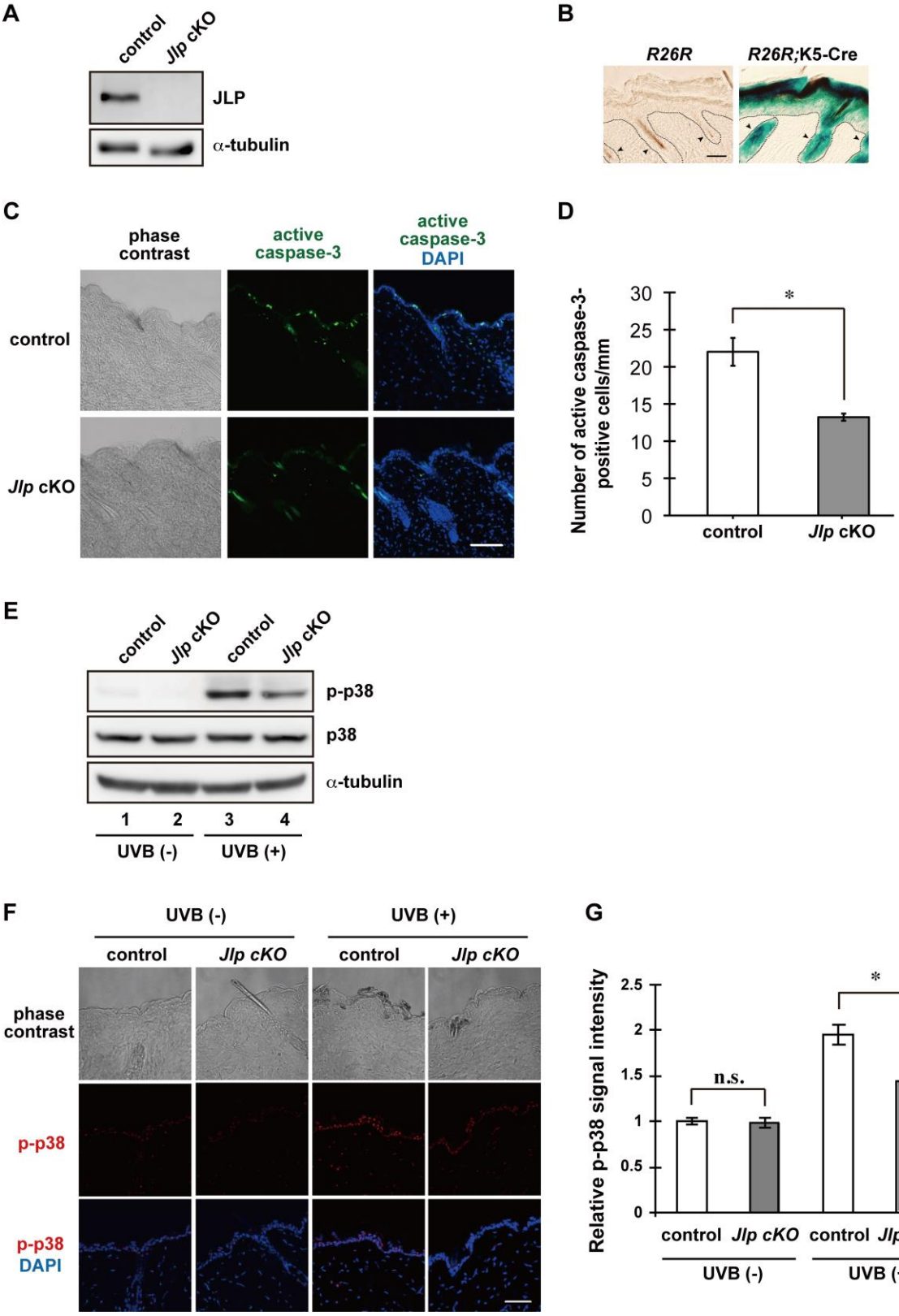
A
control
Jlp cKO
JLP
α-tubulin
B
R26R
R26R;K5-Cre
C
phase contrast
active caspase-3
active caspase-3 DAPI
control
Jlp cKO
D
Number of active caspase-3-positive cells/mm
30
25
20
15
10
5
0
*
control
Jlp cKO
E
control
Jlp cKO
control
Jlp cKO
p-p38
p38
α-tubulin
1
2
3
4
UVB (-)
UVB (+)
F
UVB (-)
UVB (+)
control
Jlp cKO
control
Jlp cKO
phase contrast
p-p38
p-p38 DAPI
G
Relative p-p38 signal intensity
2.5
2
1.5
1
0.5
0
n.s.
*
control
Jlp cKO
control
Jlp cKO
UVB (-)
UVB (+)

Figure 5. Reduced apoptosis and impaired p38 activation in the skin of keratin-specific *Jlp* cKO mice treated with UVB irradiation. **(A)** Western blotting analysis of JLP in primary keratinocytes derived from control (*Jlp*$^{flox/+}$*;K5-cre*) and *Jlp* cKO (*Jlp*$^{flox/flox}$*;K5-cre*) mice. α-tubulin was used as a loading control. **(B)** X-gal staining of skin sections from *R26R* and *R26R*;K5-Cre mice. Frozen sections (20-μm-thick) from the back skin of *R26R* and *R26R*;K5-Cre P5 mice were stained in X-gal solution for 24 hours at 37˚C. Dotted lines indicate the border between epidermis and dermis, and arrowheads point to hair follicles. Scale bar, 30 μm. **(C)** Immunohistochemical staining for active caspase-3 in control and *Jlp* cKO mice. Control and *Jlp* cKO adult mice were shaved and irradiated with UVB, and skin specimens were subjected to immunohistochemistry as in Fig. 2A. Scale bar, 100 μm. **(D)** Quantification of the results in C was performed as in Fig. 2B. Values are the mean + SEM from three independent experiments. *P < 0.05. **(E)** Western blotting analysis of p38 activation in the skin of control and *Jlp* cKO mice in response to UVB exposure. Control and *Jlp* cKO adult mice were shaved and treated with or without UVB as indicated, and cell lysates prepared from the skin samples were subjected to Western blotting as in Fig. 4A. α-tubulin was used as a loading control. **(F)** Immunohistochemical staining for p-p38 in control and *Jlp* cKO mice. Control and *Jlp* cKO adult mice were shaved and treated with or without UVB, and skin specimens were subjected to immunohistochemistry as in Fig. 4B. Scale bar, 50 μm. **(G)** Quantification of the results in F was performed as in Fig. 4C. Values are the mean + SEM from three independent experiments. n.s., not significant; *P < 0.05.

Involvement of p38 signaling in UVB-induced apoptosis

Final investigation was done to find out whether p38 signaling is required for UVB-induced apoptosis in mouse skin by using SB203580, a small molecule inhibitor of p38. As shown in Figure 6, topical treatment of UVB-irradiated mouse skin with the p38 inhibitor significantly reduced the number of active caspase-3-positive cells in the epidermis of wild-type mice, but not *Jlp* KO mice, indicating that p38 signaling plays a pro-apoptotic role in response to UVB exposure.

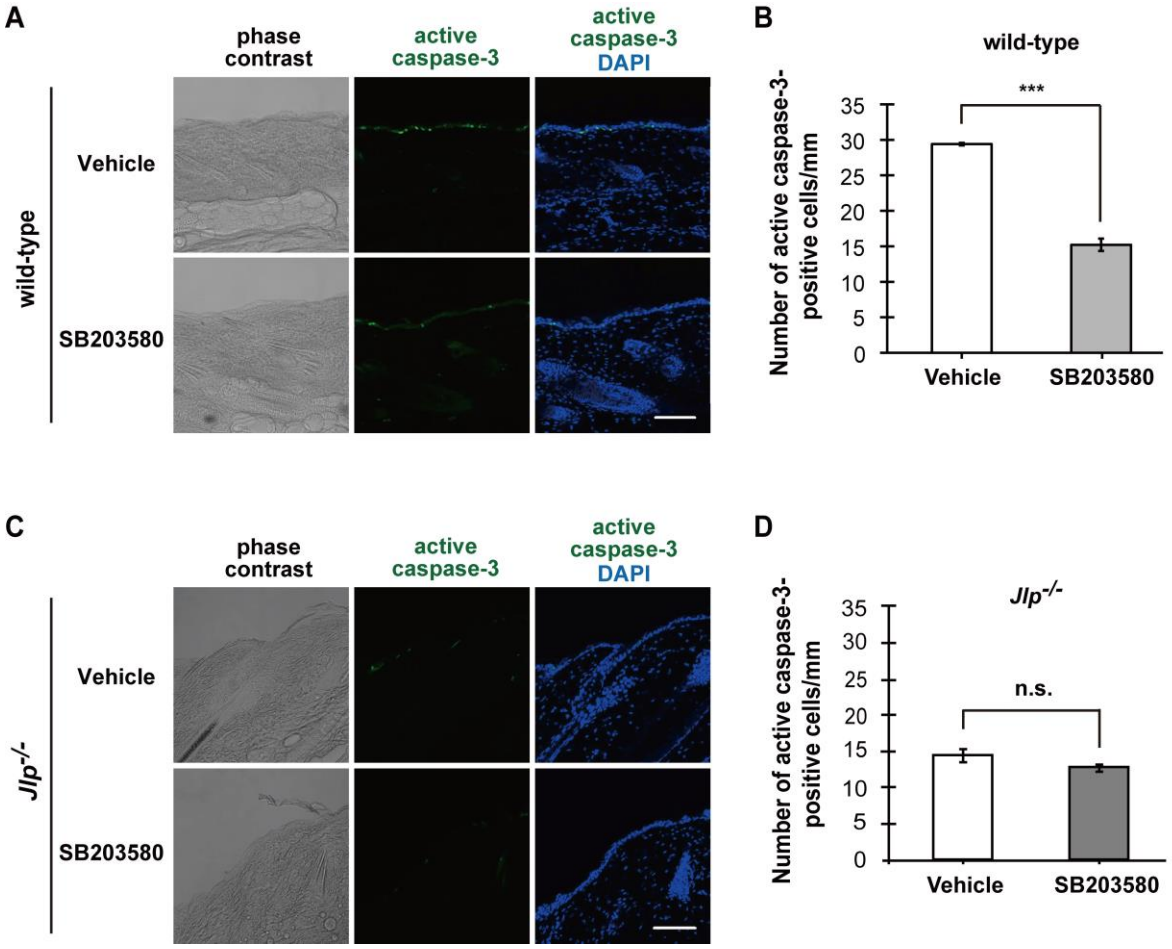

Figure 6. Involvement of p38 signaling in UVB-induced apoptosis. Immunohistochemical staining for active caspase-3 in wild-type mice (A) and *Jlp* KO mice (C). The backs of adult mice were shaved and topically treated with 40 µL of either vehicle or SB203580 (0.5 µmol) 1 hour before and just after UVB irradiation at a dose of 2.8 kJ/m^2. After 24 hours, skin specimens were subjected to immunohistochemistry as in Fig. 2A. Scale bar, 100 µm. The results in **A** and **C** were quantified in **B** and **D**, respectively. The number of active caspase-3-positive cells in the epidermis was counted over a linear distance of 10 mm, and averaged for each 1-mm interval. Values are the mean + SEM from three independent experiments. n.s., not significant;***P < 0.001.

DISCUSSION

In this study, the role of JLP in UVB-induced apoptosis in skin epidermal tissues was examined, and found that *Jlp*-deficient mice exhibit a substantially reduced apoptotic response. This is the first demonstration of a critical role for JLP in an *in vivo* response to environmental stimulation. It is also observed that conventional *Jlp* KO mice and keratinocyte-specific *Jlp* cKO mice, in which *Jlp* is disrupted in K5-expressing basal cells, exhibit almost identical effects on UVB-induced apoptosis (Figs 2, 4, 5). Thus, the lack of JLP expression in basal keratinocytes is most likely responsible for the decreased susceptibility of the *Jlp* mutant mice to UVB-induced stress. The UVB-induced activation of p38 MAPK was significantly attenuated in the epidermis of *Jlp* KO and *Jlp* cKO mice (Figs. 4C, 5G). In addition, topical application of a p38 inhibitor to the skin significantly suppressed the UVB-induced apoptosis in wild-type mice, but not in *Jlp* KO mice (Fig. 6). It is therefore likely that JLP functions as a scaffolding factor for pro-apoptotic p38 pathways following UVB stimulation in basal keratinocytes. However, it is possible that JLP and/or p38 expressed in cells or tissues other than keratinocytes also affect the regulation of the UVB-induced apoptosis independently or cooperatively. At present, the detailed mechanisms underlying UVB-induced JLP-p38 signaling remain unclear. However, considering evidence that UVB exposure stimulates the generation of reactive oxygen species (ROS) (Van Laethem *et al*., 2009), and that ROS regulate p38 activation (Dolado *et al*., 2007), UVB-induced ROS may activate JLP-mediated p38 signaling pathways. JNK/stress-activated protein kinase-associated protein 1 (JSAP1, also known as JIP3 or Sunday Driver), which is highly homologous with JLP in its sequence and domain structure, has been identified as a scaffold protein for JNK signaling pathways (Ito *et al*., 1999; Kelkar *et al*., 2000). Recently, Ongusaha *et al*. (2008) analyzed JSAP1/JIP3 knockdown cultured cells, and reported that Rho-associated kinase 1 plays an essential role in UVB-induced apoptosis by regulating JSAP1/JIP3-JNK pathways. Thus, upon UVB stimulation, the scaffold proteins JSAP1 and JLP may be responsible for the efficient activation of JNK and p38 signaling pathways, respectively, leading to apoptosis. In addition, it is also

possible that JSAP1 and JLP scaffolds are partially redundant in the regulation of JNK and/or p38 signaling pathways in response to UVB irradiation, although to date, no functional redundancy between JSAP1 and JLP has been reported. Future studies, including the analysis of keratinocyte-specific *Jsap1* cKO and *Jsap1* and *Jlp* double cKO mice, will be required to clarify this issue. The current study identified the scaffold protein JLP as a novel positive regulator of UVB-induced apoptosis. It will be interesting to determine whether *Jlp*-deficient mice exhibit an increased susceptibility to skin cancers, especially basal cell carcinoma, in response to UVB irradiation.

REFERENCES

1. Bode, A.M. & Dong, Z. (2003) Mitogen-activated protein kinase activation in UV-induced signal transduction. *Sci*. *STKE* 2003, RE2.
2. Bowden, G.T. (2004) Prevention of non-melanoma skin cancer by targeting ultraviolet-B-light signalling. *Nat. Rev. Cancer* 4, 23-35.
3. Dolado, I., Swat, A., Ajenjo, N., De Vita, G., Cuadrado, A. & Nebreda, A.R. (2007) p38 alpha MAP kinase as a sensor of reactive oxygen species in tumorigenesis. *Cancer Cell* 11, 191-205.
4. Enkhtuya R., Sato T., Wakasugi M., Tuvshintugs B., Miyata H., Sakurai T., Matsunaga T and Yoshioka K (2013) The scaffold protein JLP plays a key role in regulating ultraviolet B-induced apoptosis in mice. *Genes to Cells* in press.
5. Gantulga, D., Tuvshintugs, B., Endo, Y., Takino, T., Sato, H., Murakami, S. & Yoshioka, K. (2008) The scaffold protein c-Jun NH_2-terminal kinase-associated leucine zipper protein regulates cell migration through interaction with the G protein G (alpha 13). *J. Biochem*. 144, 693-700.
6. Ito, M., Yoshioka, K., Akechi, M., Yamashita, S., Takamatsu, N., Sugiyama, K., Hibi, M., Nakabeppu, Y., Shiba, T. & Yamamoto, K. (1999) JSAP1, a novel Jun N-terminal protein kinase (JNK) that functions as scaffold factor in the JNK signaling pathway. *Mol. Cell. Biol*. 19, 7539-7548.
7. Iwanaga, A., Wang, G., Gantulga, D., Sato, T., Baljinnyam, T., Shimizu, K., Takumi, K., Hayashi, M., Akashi, T., Fuse, H., Sugihara, K., Asano, M. & Yoshioka, K. (2008) Ablation of the scaffold protein JLP causes reduced fertility in male mice. *Transgenic Res*. 17, 1045-1058.
8. Kashef K., Lee CM., Ha JH., Reddy EP & Dhanasekaran DN (2005) JNK-interacting leucine zipper protein is a novel scaffolding protein in the Galpha13 signaling pathway. *Biochemistry*. 44(43): 14090-6.
9. Kelkar, N., Gupta, S., Dickens, M. & Davis, R.J. (2000) Interaction of a mitogen-activated protein kinase signaling module with the neuronal protein JIP3. *Mol. Cell. Biol*. 20, 1030-1043.

10. Kelkar, N., Standen, C.L. & Davis, R.J. (2005) Role of the JIP4 scaffold protein in the regulation of mitogen-activated protein kinase signaling pathways. *Mol. Cell. Biol*. 25, 2733-2743.
11. Krebs, P. & Beutler, B. (2010) Dazzle is an allele of Spag9 and results in pigmentation and sperm defects. MGI Direct Data Submission [MGI Ref ID J: 159363] Available from URL: http://www.informatics.jax.org/reference/J:159363.
12. Lee, C.M., Onésime, D., Reddy, C.D., Dhanasekaran, N. & Reddy, E.P. (2002) JLP: A scaffolding protein that tethers JNK/p38MAPK signaling modules and transcription factors. *Proc. Natl. Acad. Sci. USA* 99, 14189-14194.
13. Lippens S., Hoste E., Vandenabeele P., Agostinis P and Declercq W (2009) Cell death in the skin. *Apoptosis*. 14: 549 – 569
14. Mitchell, D.L., Haipek, C.A. & Clarkson, J.M. (1985) (6-4) photoproducts are removed from the DNA of UV-irradiated mammalian cells more efficiently than cyclobutane pyrimidine dimers. *Mutat. Res*. 143, 109-112.
15. Mizuno, T., Matsunaga, T., Ihara, M. & Nikaido, O. (1991) Establishment of a monoclonal antibody recognizing cyclobutane-type thymine dimers in DNA: a comparative study with 64M-1 antibody specific for (6-4) photoproducts. *Mutat. Res*. 254, 175-184.
16. Mori, T., Nakane, M., Hattori, T., Matsunaga, T., Ihara, M. & Nikaido, O. (1991) Simultaneous establishment of monoclonal antibodiesspecific for either cyclobutane pyrimidine dimer or (6-4) photoproduct from the same mouse immunized with ultraviolet-irradiated DNA. *Photochem. Photobiol*. 54, 225-232.
17. Nguyen Q., Lee C. M., Le A & Reddy E. P (2005) JLP Associates with Kinesin Light Chain 1 through a Novel Leucine Zipper-like Domain. J Biol Chem. 280 (34): 30185-91.
18. Ongusaha, P.P., Qi, H.H. & Raj, L. (2008) Identification of ROCK1 as an upstream activator of the JIP-3 to JNK signaling axis in response to UVB damage. *Sci. Signal* 1, ra14.

19. Sato, T., Torashima, T., Sugihara, K., Hirai, H., Asano, M. & Yoshioka, K. (2008) The scaffold protein JSAP1 regulates proliferation and differentiation of cerebellar granule cell precursors by modulating JNK signaling. Mol. Cell. *Neurosci*. 39, 569-578.
20. Sato, T., Enkhbat, A. & Yoshioka, K. (2011) Role ofplasma membrane localization of the scaffold protein JSAP1 during differentiation of cerebellar granule cell precursors. *Genes Cells* 16, 58-68.
21. Shankar, S., Mohapatra, B. & Suri, A. (1998) Cloning of a novel human testis mRNA specifically expressed in testicular haploid germ cells, having unique palindromic sequences and encoding a leucine zipper dimerization motif. *Biochem. Biophys. Res. Commun*. 243, 561-565.
22. Takaesu G., Kang JS., Bae GU., Yi MJ., Lee CM., Reddy EP & Krauss RS (2006) Activation of p38 alpha/beta MAPK in myogenesis via binding of the scaffold protein JLP to the cell surface protein Cdo. *J Cell Biol*. 175(3): 383-8.
23. Tarutani, M., Itami, S., Okabe, M., Ikawa, M., Tezuka, T., Yoshikawa, K., Kinoshita, T. & Takeda, J. (1997) Tissue-specific knockout of the mouse Pig-a gene reveals important roles for GPI-anchored proteins in skin development. *Proc. Natl. Acad. Sci. USA* 94, 7400-7405.
24. Tobin D., Hogerlinden M V and Toftgård R (1998) UVB-induced association of tumor necrosis factor (TNF) receptor 1/TNF receptor-associated factor-2 mediates activation of Rel proteins. *Proc. Natl. Acad. Sci. USA*. 95: 565–569.
25. Van Laethem, A., Garmyn, M. & Agostinis, P. (2009) Starting and propagating apoptotic signals in UVB irradiated keratinocytes. *Photochem. Photobiol. Sci*. 8, 299-308.
26. Wakasugi, M., Kasashima, H., Fukase, Y., Imura, M.,Imai, R., Yamada, S., Cleaver, J.E. & Matsunaga, T. (2009) Physical and functional interaction between DDB and XPA in nucleotide excision repair. *Nucleic Acids Res*. 37, 516-525.
27. Zhang, L.J., Bhattacharya, S., Leid, M., Ganguli-Indra, G. & Indra, A.K. (2012) Ctip2 is a dynamic regulator of epidermal proliferation and differentiation by integrating EGFR and Notch signaling. *J. Cell Sci*. 125, 5733-5744.